segmentation masks (from OAI ZIB dataset) for bone and cartilage were selected randomly from 508 scans. The 3D DESS sequence (voxel-size 0.7 x 0.35 x 0.35 mm) and manually generated expert gold-standard labels for bone and cartilage supplied by OAI investigators were used for each knee. 10 scans were randomly withheld as a test set. The Network was trained twice on two different randomly selected two small data sets of 10 scans each. As a benchmark, we also trained the network on all 400 scans with 10 scans used as the test-set.

AI: The original Mask R-CNN recognizes objects and locations by evaluating the coordinates of a bounding box in which the objects are situated in the image. Then, it applies convolution on cropped features obtained from extracted bounding boxes to extract pixel-wise masks. However, the extracted mask is not sufficiently precise around the edges of the detected objects. To improve the segmentation performance, we developed a new head network for the Mask R-CNN *(Figure 1)*. A small decoder (up-convolution layer) is added to the head to increase the spatial resolution of feature maps by up-sampling. Furthermore, higher resolution feature maps are fused into the added decoder in the header by skip connections which ensure spatial localization of features. Fusing feature maps into the decoder recovers the spatial information that has been lost in the network via a series of down-samplings for the feature extraction procedure. The backbone (ResNet) of the network, responsible for feature extraction, was initialized with weights pre-trained on the MS COCO (Microsoft Common Objects in Context) detection dataset. The performance of these two networks were evaluated and compared using the Dice similarity coefficient and Hausdorff distance for bone and cartilage.

**Results**: Accuracy metrics *(Table 1)* reveal that the maximum Hausdorff distance for all the surfaces was between 12 to 21 pixels (4-7.5 mm) for both "improved Mask RCNN" (I-Mask-RCNN). The Dice coefficient was greater than 0.95 for bones and was greater than 0.8 for cartilages. The results had strong visual face validity for the bony cortex, with only minor variation in cartilage surfaces *(Figure 2)*. Furthermore, all of the 3 I-Mask-RCNNs *(Figure 2 (c,d,e))* performed better in pixel-wise segmentation than the original Mask RCNN (Figure2 f). The two I-Mask-RCNN trained networks on 10 scans show similar pixel-wise segmentation *(Figure 2 (c and d))*, and their result is close to the I-Mask-RCNN trained on 400 scans *(Figure 2 (e))*.

**Conclusions**: The I-Mask R-CNN was able to simultaneously detect and segment multiple regions of bone and cartilage with high accuracy when trained on knee MRIs of just 10 patients. This approach shows promise for efficient automated image analysis in settings where small patient data sets and limited resources for human expert image labeling are available. The I-Mask-RCNN outperformed the original Mask R-CNN, even when trained on a small data set. Training results were similar for two different sets of 10 training scans, indicating that the method has generalization capability over different sets of data. Increasing the size of the training set to 400 scans further improved the performance only slightly. In the trade-off between the desired performance and available data, the large additional time and cost in labeling 390 more scans are unlikely justified in most situations. The proposed approach lowers the need for large training datasets, which will be beneficial for new MRI sequences and to segment other tissues in knee MRI. Our innovations to the network (adding a small decoder and embedding a higher resolution feature map into the decoder), result in a mask prediction more sensitive to image details and improve network performance around the edges of bone and cartilage. Future directions will focus on further improvements in cartilage segmentation using additional refinements of this type of network.

| Evaluation on 10 Scans TestSet | Dice | | | | Max Hausdorff distance | | | |
|---|---|---|---|---|---|---|---|---|
| | F | FC | T | TC | F | FC | T | TC |
| I-Mask-RCNN Trained on first 10 scans | 0.974 | 0.820 | 0.970 | 0.809 | 12.82 | 12.13 | 19.66 | 14.89 |
| I-Mask-RCNN trained on second 10 scans | 0.974 | 0.822 | 0.965 | 0.806 | 14.23 | 14.02 | 20.19 | 15.65 |
| I-Mask-RCNN Trained on 400 scans | 0.977 | 0.830 | 0.975 | 0.807 | 12.07 | 13.15 | 8.09 | 13.40 |
| Original Mask R-CNN Trained on 400 scans | 0.960 | 0.700 | 0.950 | 0.810 | 15.60 | 19.20 | 33.04 | 40.66 |

Quantitative evaluation results

Osteoarthritis and Cartilage

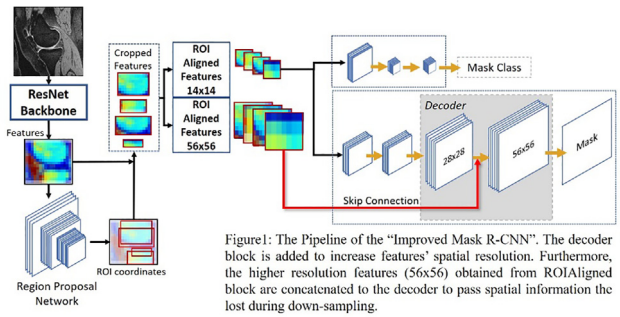


Figure1: The Pipeline of the "Improved Mask R-CNN". The decoder block is added to increase features' spatial resolution. Furthermore, the higher resolution features (56x56) obtained from ROIAligned block are concatenated to the decoder to pass spatial information the lost during down-sampling.

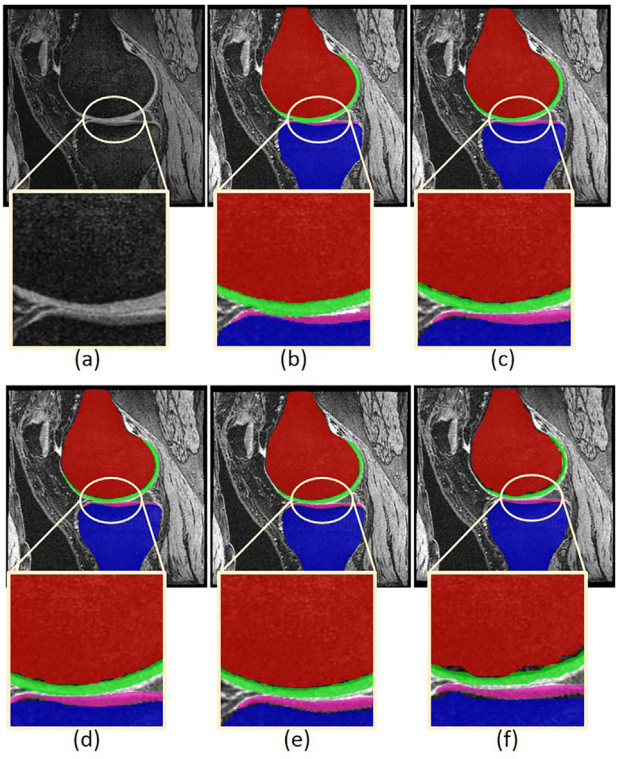


Figure2. Qualitative results and comparison between "improved Mask RCNN" and "Mask R CNN", and effect of different number of training data. a) MRI slice, b) Ground truth, c) I-Mask RCNN 10 scans (1st), d) I-Mask RCNN 10 scans (2nd), e) I-Mask RCNN 400 scans, f) Mask RCNN 400 scans

**PRESENTATION NUMBER: 423**

**DYNAMIC AND GUIDED KNEE MOTION UNDER LOADING DURING FAST MAGNETIC RESONANCE IMAGING: A NOVEL DEVICE**

N.M. Brisson [1], M. Krämer [2,3], J.R. Reichenbach [3], G.N. Duda [1]. [1] *Julius Wolff Inst., Charité – Univ.smedizin Berlin, Berlin, Germany;* [2] *Inst. of Diagnostic and Interventional Radiology, Jena Univ. Hosp., Friedrich Schiller Univ. Jena, Jena, Germany;* [3] *Med. Physics Group, Inst. of Diagnostic and Interventional Radiology, Jena Univ. Hosp., Friedrich Schiller Univ. Jena, Jena, Germany*

**Purpose**: Due to its non-invasive, direct multi-planar capabilities and excellent soft tissue contrast at high spatial resolution, magnetic resonance imaging (MRI) is a powerful modality in the evaluation of early stage osteoarthritis (OA). However, MRI of the knee is conventionally performed in static positions that do not represent the actual dynamic physiology of the joint. It is particularly relevant to evaluate musculoskeletal conditions in the context of motion and/or loading as deviations from normality can be intimately involved in the development and exacerbation of pathology and pain. For this reason, in vivo measurements of joint motion and loading are necessary to understand physiological and pathological joint mechanics. The purpose of this work was to develop a MRI-safe device for dynamic imaging of the knee joint that allows for loaded, active knee motion in the sagittal plane. Secondary objectives were to present preliminary data obtained from dynamic MRI as an example of potential device application; and to characterize the participant experience during a knee motion protocol.
**Methods:** *Device Specifications.* The knee motion/loading device was specifically designed for a 3T whole-body MRI scanner with a 60 cm diameter bore (Magnetom Prisma, Siemens) (Figure 1). The device can be used with either knee, with the participant lying supine or prone. The main components were built out MRI-safe materials (i.e., non-metallic, non-conducting, non-magnetic), including polyoxymethylene, polylactic acid filament and glass-fiber reinforced plastic. The baseplate sits atop the patient table proximally; and atop the rails within the bore of the scanner distally. The baseplate has an opening in its center through which the lower leg can move up and down. The participant is positioned with the pelvis and lower limbs on the proximal portion of the baseplate and with the upper body extended onto the padded patient table. The index knee is instrumented with a suitable flex coil. The joint's axis of rotation is aligned with that of the device, and the lower leg is secured to the leg support; the contralateral leg is placed alongside the bore. Knee motion is guided by a belt and sprocket assembly that runs along either side of the lower leg and connects to a gearbox that is put into motion by the leg support when the participant actively flexes and extends the knee. A fiber optic rotary encoder (Micronor) enables real-time monitoring of knee flexion angles. The gearbox interlinks with a rack and pinion gear, upon which weight plates can be placed to adjust the magnitude of knee loading. The rotational direction of the gears can be manipulated to elicit different types of knee muscle contraction (i.e., eccentric or concentric contraction of the quadriceps or hamstring). *MRI Data Acquisition.* MRI was acquired from one volunteer (male, 65 kg, 39 years old) without prior lower-limb injury/surgery or known musculoskeletal conditions with said 3T scanner and one element of an 8-channel multipurpose flex coil (Variety, NORAS). The participant actively performed several knee flexion-extension cycles "as slowly as possible" to accommodate the MRI data sampling rate; an external load of 10 kg was applied. Dynamic imaging was acquired using two-dimensional, dual-echo, radial gradient-echo imaging with the following parameters: 1.3 x 1.3 x 3.5 $mm^3$, 2298 Hz/pixel acquisition bandwidth, 2.4 ms and 4.9 ms TE, 8.0 ms TR, 10° excitation flip angle and a single sagittal slice, resulting in a temporal resolution of 0.5 s per frame. The datasets were reconstructed offline with MATLAB using re-gridding with iterative sampling density compensation and an optimized kernel. *Participant Reported Outcomes.* Ten male participants (age 35.0 ± 6.4 years; body mass index 23.9 ± 2.2 $kg/m^2$) without prior lower-limb injury/surgery or known lower-extremity conditions completed an active knee motion protocol with an applied external load of 35 kg. Data were acquired outside the MR environment using a specialized setup to emulate the physical constraints of the MR bore. Participants actively performed a two-minute bout of cyclic knee flexion-extension to the beat of a metronome (4 cycles/min). Subsequently, participants were asked the following questions to help characterize their experience: (1) How physically exerting was the task? (2) How much pain did you experience (and where)? (3) How much discomfort did you experience (and where)? (4) How difficult was it to keep focused on the task? Each question was scored from 0 "none/not at all" to 10 "extreme(ly)".
**Results**: *Device Specifications.* The device was designed to allow for ~35° of knee motion; i.e. from 0° (full extension) to 35° of flexion. Data acquired for the 10 participants confirmed maximum knee flexion angles of 38.6 ± 3.4°, which varied depending on foot length and ankle position (plantar/dorsiflexed). Furthermore, the device allows for the application of up to 40 kg of external load. However, due to the various components implicated in generating knee motion (i.e., sprockets, belts), the actual load actively moved by the knee muscles is less than the applied external load. This linear relationship can be expressed using the following equation: *load moved by knee muscles* = 0.14 × *external load* + 0.94. Thus, a maximum external load of 40 kg ≈ 6.3 kg (or 62 N) applied to the muscles. Depending on the moment arm (i.e., distance from the knee axis of rotation and the adjustable ankle rest), the device can impose knee moments of ~20-27 Nm (without accounting for the mass of the lower leg/foot). *MRI Data.* Dynamic MRI images acquired in sagittal orientation during active knee motion are shown in Figure 2. The images capture the knee motion without motion artifacts, allowing adequate visualization of the various knee joint structures including bones (femur, tibia, patella), articular cartilage, patellar tendon, and Hoffa fat pad. *Participant Reported Outcomes.* The self-reported scores were as follows: 5.1 ± 2.1 points for physical exertion; 0.8 ± 1.4 points for pain; 3.4 ± 3.3 points for discomfort; and 3.0 ± 1.0 points for focus. Out of the 10 participants, 3 reported pain and 5 reported discomfort in the index thigh.
**Conclusions**: The novel, MRI-safe device effectively allowed for guided knee motion during loaded, active flexion and extension. Physiologically relevant knee range of motion and moments were achieved. Dynamic MRI enabled adequate visualization of knee joint structures. In general, a knee loading protocol of extended duration (2 min) with near maximal loads (35 kg) were well tolerated by the participants; though, measurement protocols should be optimized to minimize pain and discomfort, especially in clinical populations. Moving forward, this device could be used to advance our understanding of physiological and pathological joint mechanics. Ultimately, the technology could be extended for use in clinical settings for real-time imaging of patients with knee pain and/or pathology; it could play a vital role in effectively diagnosing, monitoring and treating tissue changes that occur in OA much earlier and with greater sensitivity and specificity than static imaging.

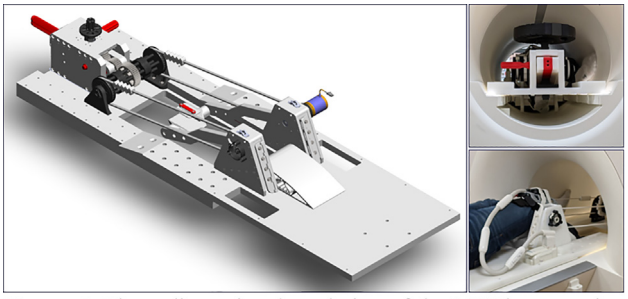

**Figure 1.** Three-dimensional rendering of the MRI knee motion device (left) and pictures of the device in the scanner (right).

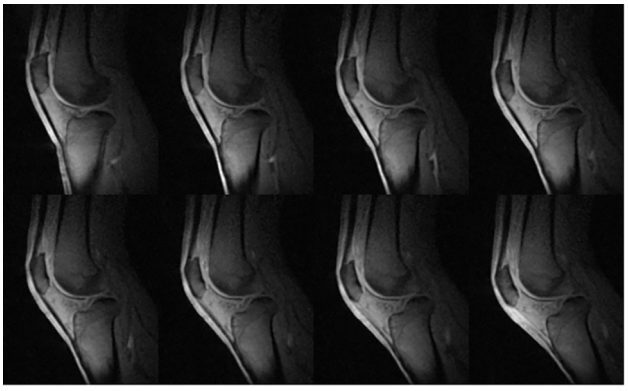

**Figure 2.** Eight selected frames illustrating the extension portion of an active knee flexion-extension cycle with 10 kg external load acquired with two-dimensional radial gradient-echo imaging. Shown is the second echo acquired at a TE of 4.9 ms.